

Localization of Breast Tumor Using Four Elements UWB Wearable Antenna

Mazhar B. Tayel¹, Tamer G. Abouelnaga², and Nehad M. Badran³

¹Department of Electrical Engineering
Faculty of Engineering Alexandria, University-Alexandria, Egypt
profbasyouni@gmail.com

²Microstrip Circuits Department
Electronics Research Institute ERI, Cairo, Egypt
tamer@eri.sci.eg

³Department of Electrical and Computer Engineering
Higher Institute of Engineering and Technology-Kafr Elsheikh, Egypt
nehadbdran1990@gmail.com

Abstract – In this paper, four wearable UWB antennas are designed to detect and locate tumor cells placed within a heterogeneous phantom at different positions. The proposed antenna is operated within the 4.90 GHz to 15.97 GHz bandwidth range. It is fabricated, measured, and nearly matched between measured and simulated results. A cavity is formulated to back each antenna within the proposed detection system for increasing penetration and gain of propagated electromagnetic waves of the antenna design. The S-parameter of the proposed system was used to detect and locate a small tumor. The SAR results show that the absorbed power by the breast phantom tissues satisfies the IEEE standards which confirms the appropriateness of the proposed antennas for breast cancer early detection and localization system.

Index Terms – cavity, heterogeneous phantom, specific absorption rate (SAR), wearable UWB antenna.

I. INTRODUCTION

In December 2020, the International Agency for Research on Cancer (IARC) announced that breast cancer has overtaken the most diagnosed type of cancer in the world. In 2021, the World Health Organization (WHO) declared breast cancer to be the most common type of cancer globally, accounting for 12% of all new cases of cancer [1]. Breast cancer arises in the glandular tissue of the breast in ducts (85%) and lobules of (15%) and is called at this stage “in situ”. This stage (stage 0) has a low chance of spreading and converting to metastasis. After a while, this stage may progress and strike surrounding tissues and then spread to nearby lymph nodes and become a regional metastasis or to other organs in the human body and become distant metastasis [2]. Tumor size is a strong predictor of long-term mor-

tality [3]. It is recommended to detect breast cancer at or less than 2 cm [4].

Breast microwave imaging (MI) in literature is split into microwave breast imaging several techniques and image reconstruction algorithms [5]. Different methods for several techniques in breast MWI (breast cancer early detections) were used. Table 1 shows many early breast cancer UWB antennas and compares them. The first method of breast MWI relied on an antenna array. There are various compositions from antenna arrays are proposed in literature papers, and ranked as hemispherical, enclosed, and planer arrays [5]. In [6], constructed a compact, single polarization, flexible UWB antenna array, in a configuration identical to that of a bra for breast cancer detection. In [7], established a compact, single and dual polarization, flexible UWB antenna array, in a structure related to that of a bra for breast cancer detection and significantly better penetration for propagated electromagnetic waves by utilizing a reflector with the arrays. In [8], formulated clinical model as a wearable interface for a case consisting of multi-static time-domain pulsed radar and flexible antenna array inundated in bra. The clinical model is highly cost-effective and related to the normal table model. The regular difference for the data of the reflection coefficient for flexible microstrip antenna array at 1.5 GHz was used to locate and detect the tumor at thirteen numerous places in the human breast [9]. The second method of MWI of the breast depended on a single antenna element. These antennas include Vivaldi antennas, monopole antennas, and bowtie antennas, in addition to fractal and horn antennas [5]. In [10], a wearable microstrip patch UWB antenna as a new design had demonstrated to detect early tumors with enlarged bandwidth from 1.6 GHz to 11.2 GHz. In [11], a compact flexible single-element UWB antenna

Table 1: Comparison among early breast cancer detection antennas

Reference	Single element size (mm ²)	No. of elements	ϵ_r	Substrate thickness (mm)	Length of single element/ λ (mm)	BW (GHz)	$\Delta f/f_0$
[6]	18 × 18	16	3.5	0.1	0.250	2 – 5	0.86
[7]	20 × 20	16	3.5	0.1	0.280	2 – 4	0.67
[8]	20 × 20	16	3.5	0.1	0.280	2 – 4	0.67
[9]	58.43 × 26.45	4	2.64	2.2	0.470	1.45 – 1.54	0.06
[10]	70 × 60	2	1.6	1.6	0.740	1.6 – 11.2	1.5
[11]	22 × 20	1	3.5	0.05	0.410	2 – 4	0.67
[12]	25 × 36	1	3.4	0.16	0.730	2 – 4	0.67
In this paper	28 × 20	4	2.9	0.1016	0.830	4.90 – 15.97	1.06

with an inhomogeneous breast phantom was presented for MWI and tumor early detection. It was operated in the range of 2 to 4 GHz while having a size of 20 × 22 mm². Kapton substrate with a relative permittivity of 3.5 has been used as a substrate. In [12], a compact flexible monopole single-element UWB antenna with an inhomogeneous breast phantom for breast cancer detection Kapton polyimide using a CST simulator and MEMS technology with biological breast tissues. It was operated in the range of S-Band (2-4 GHz) while having a size of 25 × 36 mm². All the mentioned researches suffer from small (single element length/ λ) and low fractional bandwidth value of single element antenna.

In this paper, Four UWB wearable antennas and four cavities are suggested for the breast phantom examination to detect and locate tumor tissues inside the human breast. Firstly, the evolution of a single UWB wearable antenna is accomplished in four steps and verified. Secondly, the cavity is utilized around each wearable antenna for significantly nicer penetration for radiated electromagnetic waves. Finally, the proposed phantom with and without tumor tissues is simulated with the proposed detection system which is consisted of four UWB wearable antennas and a cavity around each antenna. S-parameters from the single-element antenna are reported by using CST Microwave Studio 2020 and are compared with the measured results for the fabricated proposed antenna by using Vector Network Analyzer (VNA). S₁₁ from the single-element antenna can detect and diagnose the presence of malignant cells. The tumor position is identified by other reflection coefficients of all antennas. SAR estimation is also investigated for the proposed phantom. The proposed detection system indicates that the two processes of early detection and localization for tumors 3 mm in size inside a human breast are possible.

II. The PROPOSED ANTENNA DESIGN

A. Antenna element

The antenna design is an important part of the overall performance of microwave imaging systems. Breast microwave imaging systems need to antenna element

which radiates pulses over a wide range of frequencies and operates in the Ultra-Wideband (UWB) that the Federal Communication Commission (FCC) assigned a bandwidth of (3.1 to 10.6 GHz) for measurements, communications, and radar [13].

The growth of the proposed antenna configuration is accomplished in the four stages as illustrated in Fig. 1. The structure of the octagon antenna element with a partial ground plane is altered for the desired operating bandwidth. The structure of the octagon's antenna element is modified from stage 1 to stage 2. The conclusions of the return loss of the development process are demonstrated in Fig. 2. The return loss of the designed octagon antenna element with the partial ground plane in stage 1 is ≤ -10 dB for the frequency range of 8.7897 GHz to 17.11 GHz. In stage 2, the number of partial octagons is increased in radiating patch to enhance the return loss. Subsequently, the return loss is accomplished for the frequency range of 8.6159 GHz to 16.599 GHz. In stage 3, a rectangular shape structure is added to the ground plane. The resonating behavior of the antenna is altered by this addition. The result of this improvement is visualized in the return loss graph in Fig. 2. In this stage the lower frequency range of the return loss has improved. Then the modified antenna covered the Ultra-wideband region from 5.1315 GHz to 16.272 GHz. The rectangular-shaped structure is replaced with a radial stub in stage 4. The shape modification considers the like self-similarity and slots which played an important role to widen the bandwidth. Now, this replacement shifted the bandwidth from 5.1315 GHz to 4.9007 GHz at the lower frequency and from 16.272 GHz to 15.968 GHz at the higher frequency. The optimized size of the proposed antenna is 28 mm × 20 mm. The radiating patch and ground plane are printed on the substrate. The Ultra-Lam 3850 dielectric constant of 2.9 and thickness of 0.1016 mm is used as an antenna flexible substrate. The proposed antenna structure is shown in Figs. 3 (a) and (b). The fabricated antenna is tested with Vector Network Analyzer (VNA) for validation purposes in Fig. 3 (c). Table 2 shows the optimized dimensions of the proposed antenna. Figure 4

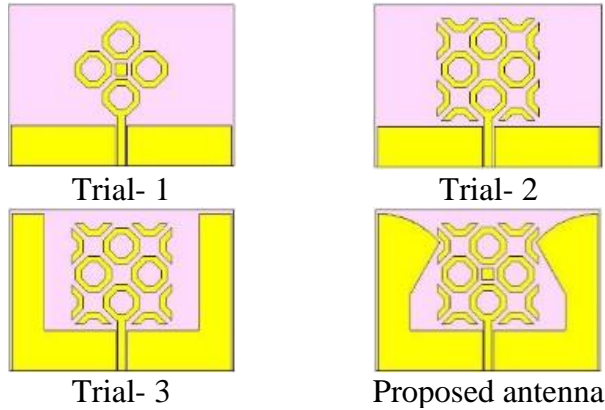


Fig. 1. Evolution stages for designing the proposed antenna.

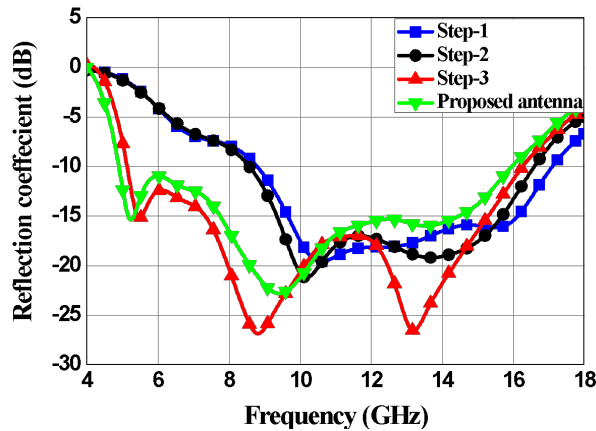


Fig. 2. The return loss results of the evolution process of the proposed antenna.

shows the fabricated antenna top and bottom views. The return loss of the fabricated antenna and its simulated counterpart is shown in Fig. 5. These results are closely matched. Variation in the simulation and measurement results between 8-11 GHz shown below might be due to fabrication errors and accuracy parameters or to the soldering used in linking the SMA connector to the feedline of the antenna and the SMA connector effect. Figure 6 shows the 3D radiation pattern of the antenna; the antenna has an omnidirectional radiation pattern. Also, the beam width (angular width) is 58.8%. Figure 9 shows the radiation pattern in the x - z plane. Table 3 shows the comparison among the evolution stages of the proposed UWB wearable antenna.

B. Effect of antenna bending

The wearable antennas are required to be bent as human breast shape. To investigate the bending effect on the proposed wearable UWB antenna, the antenna is bent around foam cylinders with different radii at 30, 60, 90,

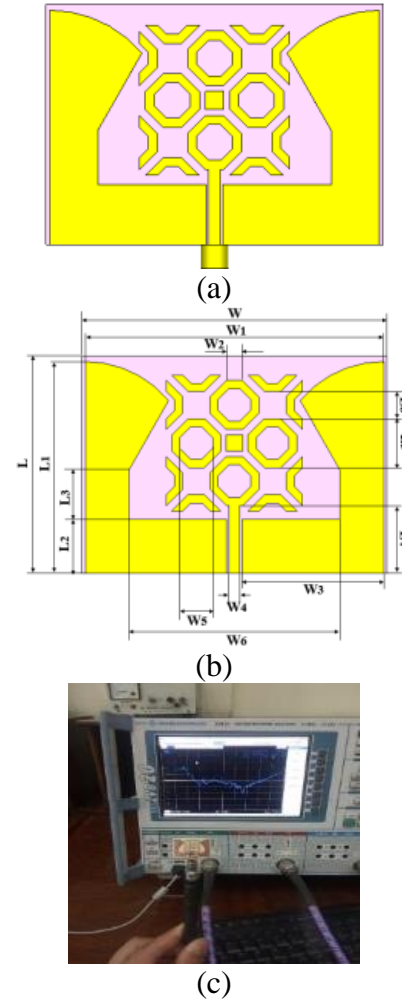


Fig. 3. (a) The proposed antenna structure. (b) The proposed antenna dimension. (c) The measurement setup.

120, and 180 mm [14, 15]. The 2D antenna representation as flat and with regards to the bending angles are depicted in Fig. 8. The return loss results of the different radii of bending are shown in Fig. 9.


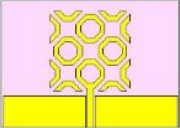
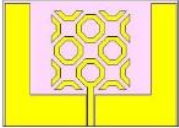

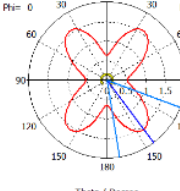
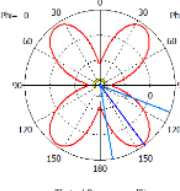
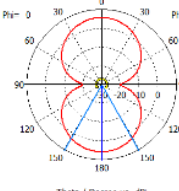
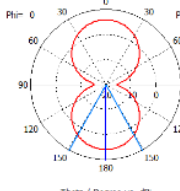
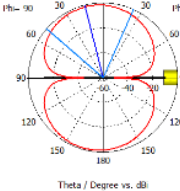
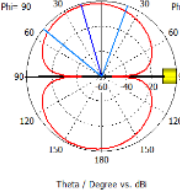
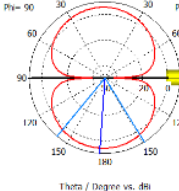
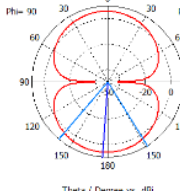
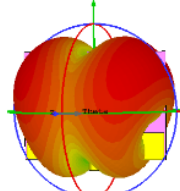
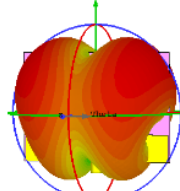
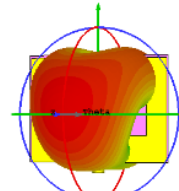
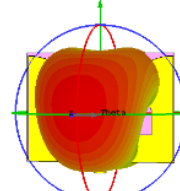
C. Cavity-backed UWB wearable bent antenna

The concept of cavity-backed antenna is creating reflectors on all sides of the antenna except the front side of

Table 2: The proposed antenna dimensions

Par.	W	W ₁	W ₂	W ₃	W ₄
Dim. ([0-9] mm)	28	27.4	1.5	13	1
Par.	W ₅	W ₆	L	L ₁	L ₂
Dim. (mm)	3	19.4	20	19.5	5
Par.	L ₃	L ₄	L ₅	L ₆	θ
Dim. (mm)	4.5	6.5	4.5	2.5	50

Table 3: The proposed antenna parameters

	Stage 1	Stage 2	Stage 3	Proposed antenna	
Antenna Shape					
Bandwidth (GHz)	8.79 – 17.11	8.5871 – 16.61	5.131 – 16.275	4.9 – 15.97	
Gain (dBi)	3.69	3.81	5.63	5.81	
Directivity (dBi)	3.72	3.86	5.66	5.85	
3dB BW (degree)	60.6	59.6°	59.2	58.8	
Radiation Efficiency (%)	99.21	98.88	99.27	98.93	
Total Efficiency (%)	94.46	96.00	98.88	98.42	
Radiation Pattern	E - Plane				
	H - Plane				
	3D				

it [16] and increasing the gain of the antenna. The dimension of the proposed cavity structure is 40 mm x 36 mm x 13.1618194 mm. The front side of the cavity structure is shown in Fig. 10 (a). The top side of the cavity structure is shown in Fig. 10 (b). Figure 11 shows the return loss

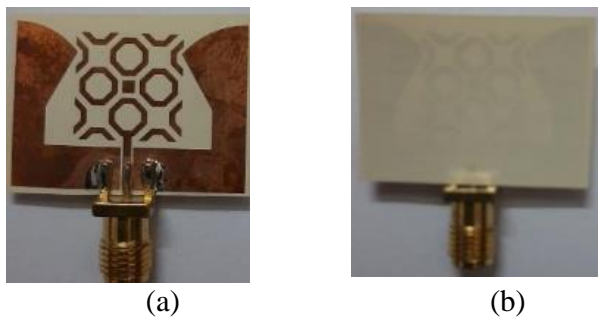


Fig. 4. The fabricated antenna (a) top view and (b) back view.

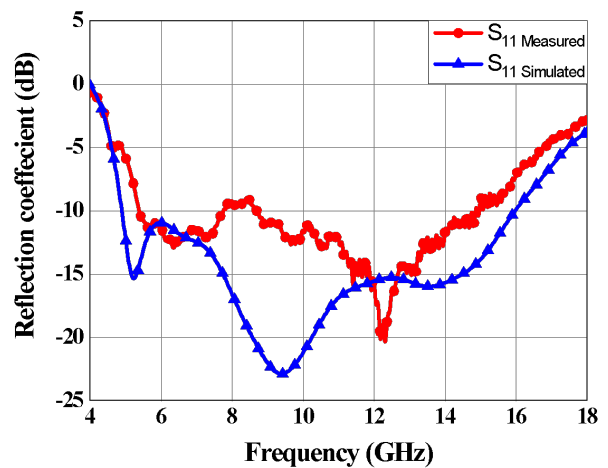


Fig. 5. The return loss of the fabricated antenna and simulated antenna.

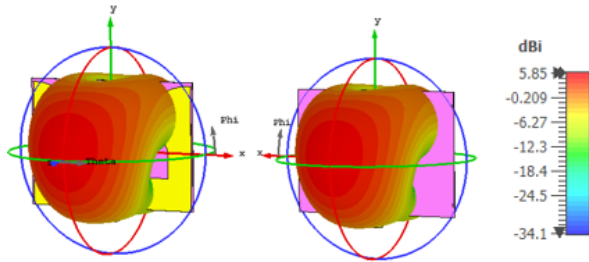


Fig. 6. The radiation pattern of the proposed antenna with metamaterial from the front side and backside.

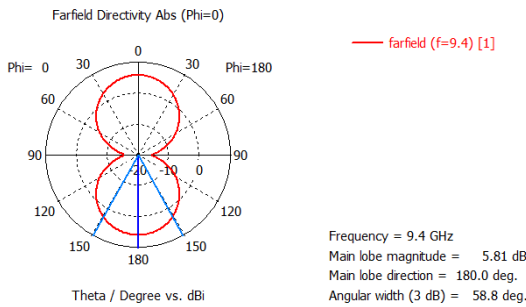


Fig. 7. The XZ plane of the radiation pattern.

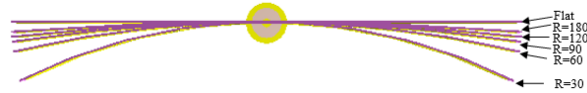


Fig. 8. The 2D flat antenna and bending around a radius at 30, 60, 90, 120, and 180 mm.

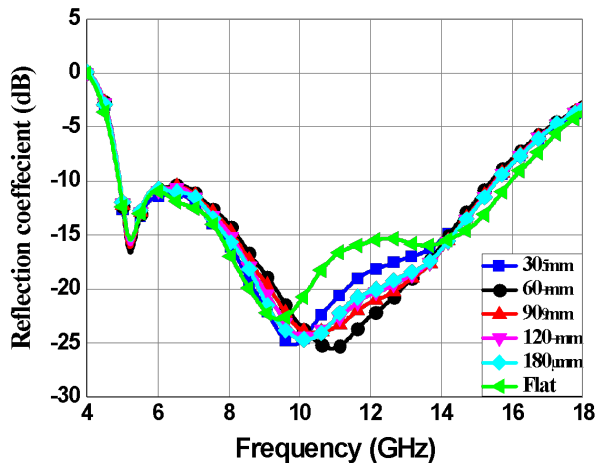


Fig. 9. The return loss results at different bending radii.

results of bending the antenna with a radius of 90 mm without a cavity and cavity-backed antenna. Figure 12 shows the 3D radiation pattern of the cavity-backed an-

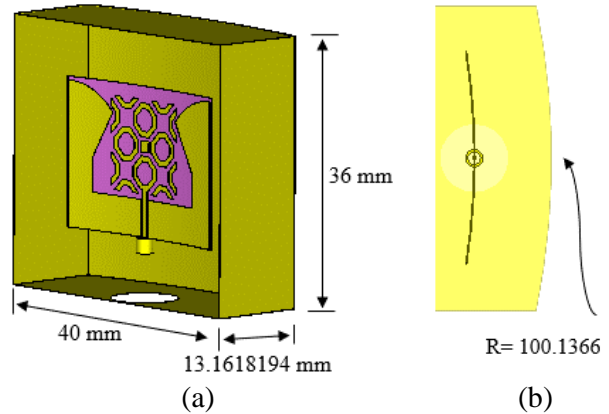


Fig. 10. (a) The front side of the cavity structure. (b) The top side of the cavity structure.

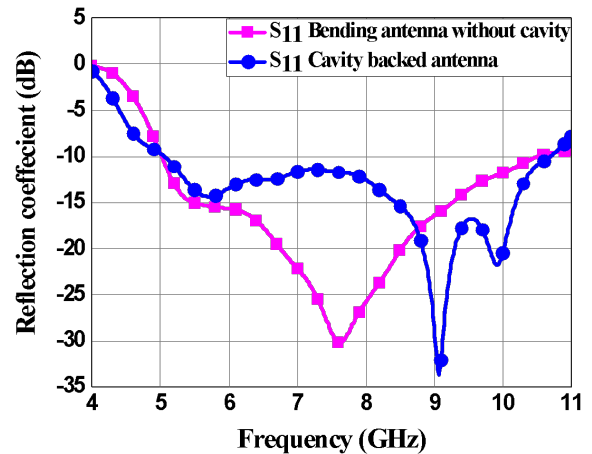


Fig. 11. The return loss of bending antenna without cavity and cavity-backed antenna.

tenna, one noticed that the cavity increases the directivity of the wearable antenna from 5.852 dBi to 10.65 dBi and the beam width (angular width) changes from 58.8% to 50.3% at the same frequency 9.4 GHz. The gain changes from 5.805 dBi to 10.6 dBi. Figure 13 shows the radiation pattern in the x-z plane.

III. THE PROPOSED DETECTION SYSTEM

A. Breast phantom

A heterogeneous phantom is used. It is structured in a 3-D hemisphere shape. It consists of various layers of breast tissues (skin, fat, glandular tissues, and tumors). Figure 14 shows the different layers of the proposed heterogeneous phantom. Tables 4 and 5 show the dimensions of the different layers of the breast and the electromagnetic parameters (Thickness T , outer radius R_{out} (mm), inner radius R_{in} (mm), Relative permittivity (ϵ),

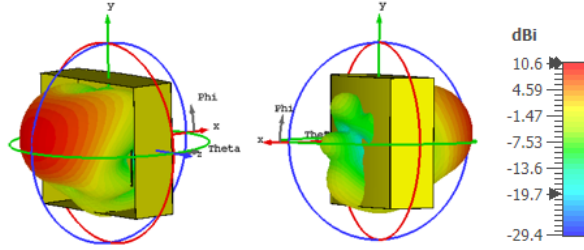


Fig. 12. The radiation pattern of the proposed antenna with cavity from the front side and backside.

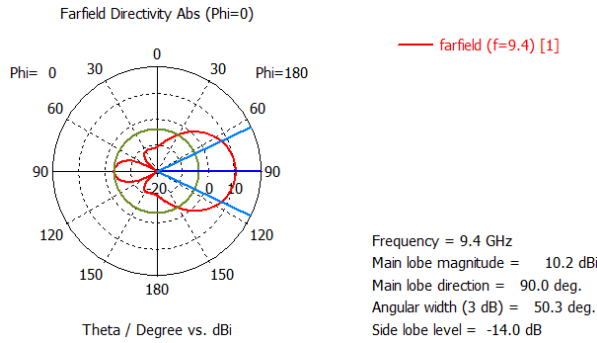


Fig. 13. The XZ plane of the radiation pattern.

conductivity (σ), Density(ρ), Specific heat capacity (cp), and Thermal conductivity (k) respectively [17, 18].

B. Antennas setup

Four antennas are bent around the human breast. Antenna 1 and antenna 3 are opposite to each other, antenna 2 and antenna 4 are opposite to each other, each antenna far distance from the breast skin by 38 mm, and the radius of the bending of the antenna is equal to 90 mm. The distance between the cavity and the antenna is 10 mm. The radius of the bent cavity is 100 mm. Figure 15 shows the front and top sides positions of the proposed cavities backed by bent antennas and the breast phantom.

IV. RESULTS AND DISCUSSION

A. Tumor detection

Breast cancer originates in the glandular tissue of the breast, so we always try to detect and locate the tu-

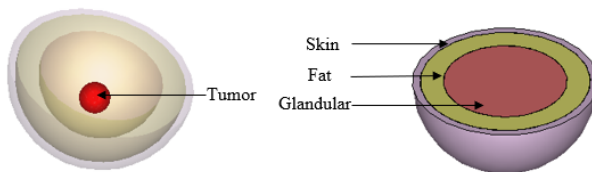


Fig. 14. Different layers of the proposed heterogeneous phantom.

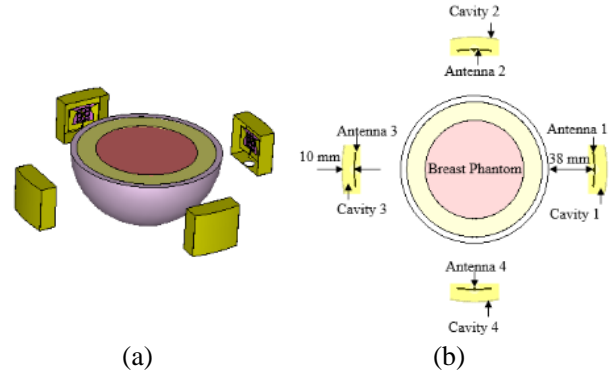


Fig. 15. (a) The front side of the detection system, (b) The top side of the detection system.

Table 4: Breast different layers of breast dimensions

Tissues	T (mm)	R_{out} (mm)	R_{in} (mm)
Skin	5	60	55
Fat	15	55	40
Glandular	40	40	0

mor early within this glandular tissue (stage I), where it is less likely to spread. Firstly, the proposed system is operated in the case of healthy breast tissues free of any tumors and then reports the coupling coefficients of the four proposed antennas for comparison with the coupling coefficients in the situation of unhealthy tissue containing tumors. Next, we split the glandular layer within the proposed breast into four quadrants: I, II, III, and IV. We hypothesized a tumor in the first quadrant, simulated the proposed system, and recorded the results again. Afterward, the tumor was eliminated from the first quadrant and immersed in another quadrant, and the system was simulated and the results were recorded again. The simulations were performed 4 times for each position of 4 tumor locations: P1 in quarter I, P2 in quarter II, P3 in quarter III, and P4 in quarter IV. The phantom quadrants and the positions of tumors are shown in Fig. 16.

The reflection coefficients S_{11} , S_{22} , S_{33} , and S_{44} for five cases, healthy breast tissue cases, and the four positions of the tumor in the unhealthy tissue at 9.34 GHz are presented in Table 6 and Fig. 17–20, respectively. Figure 21 shows the coupling between the four adjacent antennas, where a very low coupling, very good isolation, and good spatial diversity are achieved, where the coupling coefficients S_{12} is -47.57 dB at 9.47 GHz, S_{13} is -48 dB at 8.35 GHz and S_{14} is -47.32 dB at 9.47 GHz.

In the absence of a tumor case, the coupling coefficient S_{11} is equal to S_{44} and S_{22} is equal to the coupling coefficient S_{33} . In the case of a tumor in the first quadrant (P1), the values of S_{22} and S_{44} remain equal to the same values as it was in the absence of a tumor but the values

Table 5: The electromagnetic parameters of the proposed phantom

Tissues	Dielectric properties		ρ (Kg/m ³)	cp (J/K/Kg)	k (W/K/m)
	ϵ (F/m)	σ (S/m)			
Skin	36	4	1085	3765	0.4
Fat	9	0.4	1069	2279	0.3
Glandular	11–15	0.4–0.5	1050	3600	0.5
Tumor	50	4	1050	3600	0.5

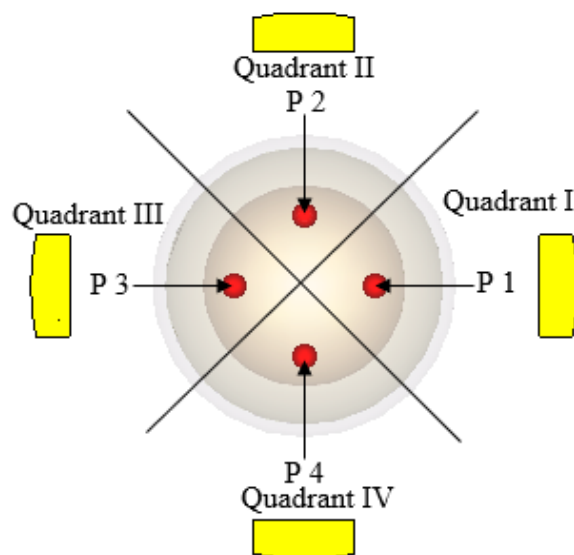
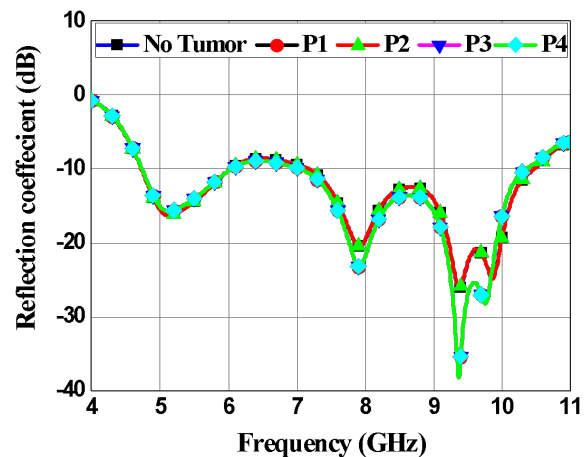


Fig. 16. The phantom splitting and the positions of tumors.

Table 6: The reflection loss of the five cases

	Tumor positions				
	No tumor	P1	P2	P3	P4
S_{11} (dB)	25.5	34.5	25.4	34.7	25.4
S_{22} (dB)	28.3	28.1	66.4	28.1	61.9
S_{33} (dB)	28.3	63.6	28	68.5	28
S_{44} (dB)	25.5	25.4	34.5	25.4	34.3

of S_{11} and S_{33} change so that the value of S_{33} is greater than the value of S_{11} and less than 65 dB. In the case of a tumor in the second quadrant (P2), the values of S_{11} and S_{33} remain equal to the same values as it was in the absence of a tumor but the values of S_{22} and S_{44} change so that the value of S_{22} is greater than the value of S_{44} and greater than 65 dB. In the case of a tumor in the third quadrant (P3), the values of S_{22} and S_{44} remain equal to the same values as it was in the absence of a tumor but

Fig. 17. The reflection coefficients S_{11} for all cases.

the values of S_{11} and S_{33} change so that the value of S_{33} is greater than the value of S_{11} and greater than 65 dB. In the case of a tumor in the fourth quadrant (P4), the values of S_{11} and S_{33} remain equal to the same values as it was in the absence of a tumor but the values of S_{22} and S_{44} change so that the value of S_{22} is greater than the value of S_{44} and less than 65 dB.

The simulations were done at different distances between the antenna and the cavity at 5, 10, and 15 mm but the best results were at 10 mm. Many parameters affect that distance as antenna resonance frequency and the tumor positions.

B. Specific Absorption Rate (SAR) analysis

Faraday's law states that the magnetic field of the coil transmits radio frequency energy and generates an electric field within the tissues of the human body and the absorbed radio frequency energy is recycled into heat [19]. Therefore, tissue heating has health effects on patients as a result of their exposure to radio frequency, and these effects can be measured and controlled by the so-called Specific Absorption Rate (SAR) [20]. The Specific Absorption Rate (SAR) is a measure of the absorption rate of Radio Frequency (RF) power by biological tissue while it is exposed to Radio Frequency (RF) energy. For calculating the SAR value, we need a volume, its mass has 1 gram or 10 grams and this volume must be

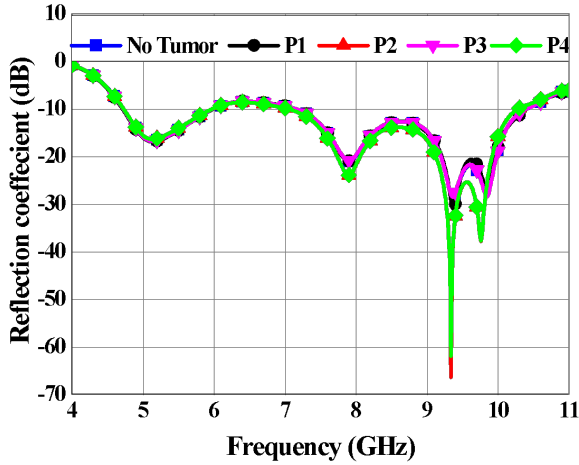


Fig. 18. The reflection coefficients S_{22} for all cases.

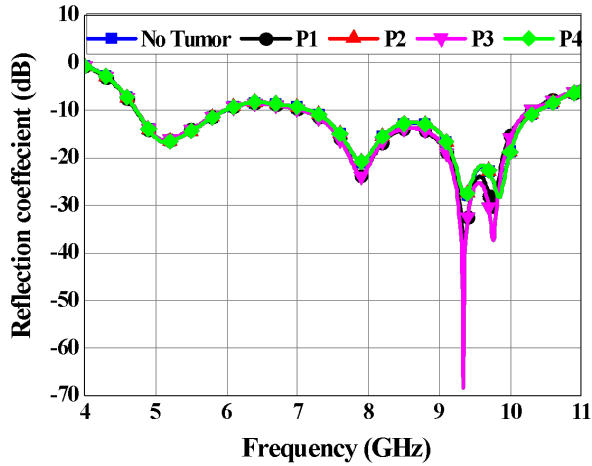


Fig. 19. The reflection coefficients S_{33} for all cases.

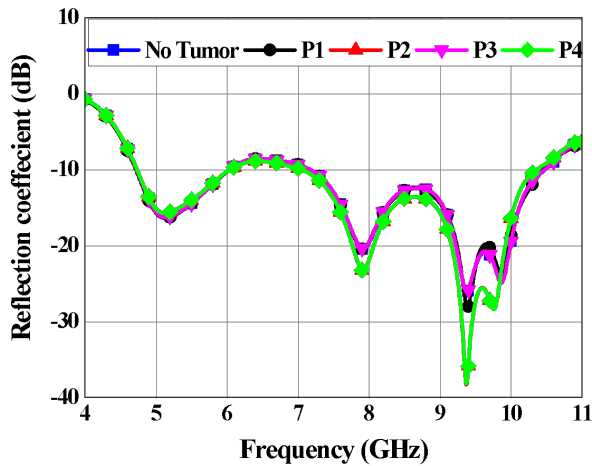


Fig. 20. The reflection coefficients S_{44} for all cases.

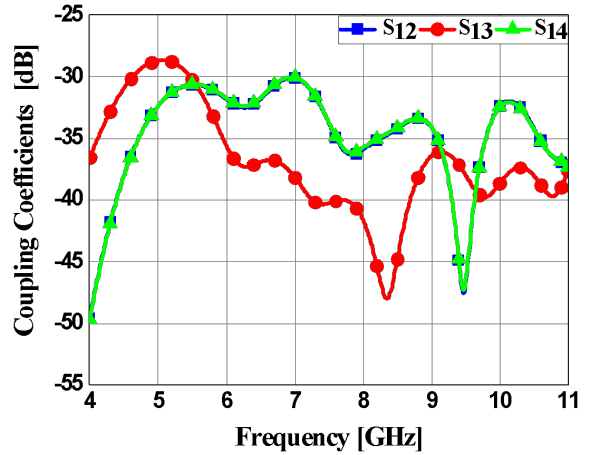


Fig. 21. The coupling coefficients S_{12} , S_{13} , and S_{14} for the proposed detection system.

a cubic shape and contains the peak electric field by the condition of the IEEE Standard 1528 [21].

The local SAR is the value of SAR at each point inside the phantom tissues [W/Kg] and it is defined by Eq.1 [20]:

$$SAR_{local}(r, \omega) = \frac{\sigma(r, \omega) |E(r, \omega)|^2}{2\rho(r)} \quad (1)$$

The average SAR is the integral of the local SAR at each point on the cube and then divided by the mass of the cube and it is defined by Eq.2:

$$SAR_{average}(r, \omega) = \frac{1}{v} \int \frac{\sigma(r, \omega) |E(r, \omega)|^2}{2\rho(r)} dr, \quad (2)$$

where $\sigma(r, \omega)$ is the conductivity of the material of the phantom [S/m], $\rho(r)$ is the mass density of the tissue [Kg/m³], $E(r, \omega)$ is the electric field [V/m], r is the position vector, and ω is the frequency.

The SAR analysis of the heterogeneous phantom using the proposed bending antenna system is carried out

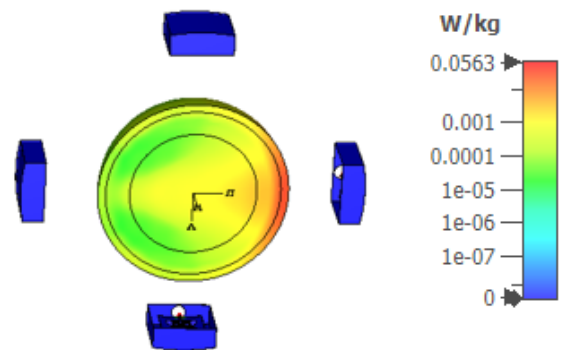


Fig. 22. The maximum spatial average SAR value using 1g.

by the Biomedical environment of the CST. The spatial average of SAR values of 1 g and 10 g volumetric samples for heterogeneous phantoms are analyzed at 9.34 GHz frequency. These results (Fig. 22) show that the maximum spatial average SAR value using 1g and 10g samples are 0.0563 [W/Kg] and 5.2×10^{-4} [W/Kg] respectively at 0.5 W at the phantom. These values are significantly below the maximum limit assigned by Federal Communications Commission (FCC) in the United States, which is 1.6[W/Kg] averaged over 1 g volume, and the standard in Europe, is 2 [W/Kg] averaged over 10 g volume.

V. CONCLUSION

A configuration and implementation of a UWB wearable antenna were introduced to detect the malignant tissues inside the human breast. The UWB wearable antenna bandwidth extends from 4.90 GHz to 16 GHz. Good agreement was achieved between measured and simulated results. The proposed cavity-backed antenna achieved high directivity, high gain, and reasonable beamwidth. A heterogeneous breast phantom with a 3mm tumor radius was tested at 9.34 GHz for tumor detection and localization processes. SAR results were investigated using 1g and 10g standards and had shown the appropriateness of the proposed antennas for breast cancer early detection and localization system.

REFERENCES

- [1] WHO | World Health Organization.
- [2] U.S. Breast Cancer Statistics.
- [3] S. A. Narod, "Tumour size predicts long-term survival among women with lymph node-positive breast cancer," vol. 19, pp. 249-253, 2012.
- [4] A. B. Miller, C. Wall, C. J. Baines, P. Sun, T. To, and S. A. Narod, "Twenty-five-year follow-up for breast cancer incidence and mortality of the Canadian National Breast Screening Study: randomized screening trial," *Obstetrical & Gynecological Survey*, vol. 69, pp. 329-330, 2014.
- [5] H. M. El Misilmani, T. Naous, S. K. Al-Khatib, K. Y. Kaban, "A survey on antenna designs for breast cancer detection using microwave imaging," *IEEE Access*, vol. 8, pp. 102570-102594, 2020.
- [6] H. Bahrami, E. Porter, A. Santorelli, B. Gosselin, M. Popovic, and L. A. Rusch, "Flexible sixteen monopole antenna array for microwave breast cancer detection," *36th Annual International Conference of the IEEE Engineering in Medicine and Biology Society*, Chicago, IL, pp. 3775-3778, Aug. 2014.
- [7] H. Bahrami, E. Porter, A. Santorelli, B. Gosselin, M. Popovic, and L. A. Rusch, "Flexible 16 antenna array for microwave breast cancer detection," *IEEE Transactions on Biomedical Engineering*, vol. 62, no. 10, pp. 2516-2525, Oct. 2015.
- [8] E. Porter, H. Bahrami, A. Santorelli, B. Gosselin, L. A. Rusch, and M. Popović, "A wearable microwave antenna array for time-domain breast tumor screening," *IEEE Transactions on Medical Imaging*, vol. 35, no. 6, pp. 1501-1509, Jun. 2016.
- [9] M. Mamun U. Rashid, A. Rahman, L. C. Paul, J. Rafa, B. Podder, and A. K. Sarkar, "Breast cancer detection & tumor localization using four flexible microstrip patch antennas," *International Conference on Computer, Communication, Chemical, Materials, and Electronic Engineering (IC4ME2)*, Rajshahi, Bangladesh, Jul. 2019.
- [10] F. Alsharif and C. Kurnaz, "Wearable microstrip patch ultra-wide band antenna for breast cancer detection," *41st International Conference on Telecommunications and Signal Processing (TSP)*, Athens, Greece, Jul. 2018.
- [11] A. Afyf, L. Bellarbi, A. Achour, N. Yaakoubi, A. Errachid, and M. A. Sennouni, "UWB thin film flexible antenna for microwave thermography for breast cancer," *International Conference on Electrical and Information Technologies (ICEIT)*, Tangiers, Morocco, May 2016.
- [12] A. Afyf, A. Elouerghi, M. Afyf, M. A. Sennouni, and L. Bellarbi, "Flexible wearable antenna for body centric wireless communication in S-band," *International Conference on Electrical and Information Technologies (ICEIT)*, Rabat, Morocco, Mar. 2020.
- [13] T. Abouelnaga and E. A. Abdallah, "Ultra-compact UWB power divider for 5G Sub-6 GHz wireless communication system," *International Journal on Communications Antenna and Propagation (IRECAP)*, vol. 12, no. 2, pp. 90-97, 2022.
- [14] S. J. Chen, B. Chivers, R. Shepherd, and C. Fumeaux, "Bending impact on a flexible ultrawideband conductive polymer antenna," *International Conference on Electromagnetics in Advanced Applications (ICEAA)*, Turin, Italy, Sep. 2015.
- [15] A. I. Hammoodi, H. Al-Rizzo, A. A. Isaac, A. S. Kashkool, K. Gamer, and H. Khaleel, "Studying the effect of bending on the performance of flexible dual-band microstrip monopole antenna," *IEEE Conference on Antenna Measurements & Applications (CAMA)*, Syracuse, NY, Oct. 2016.
- [16] D. Awan, S. Bashir, and W. Whittow, "High gain cavity backed UWB antenna with and without band notch feature," *Loughborough Antennas & Propagation Conference (LAPC)*, Loughborough, UK, Nov. 2013.

- [17] M. Abdel-Haleem, T. Abouelnaga, M. Abo-Zahhad, and S. Ahmed, "Enhancing microwave breast cancer hyperthermia therapy efficiency utilizing fat grafting with horn antenna," *International Journal of RF and Microwave Computer-Aided Engineering*, vol. 31, no. 6, pp. 1-13, 2021.
- [18] P. T. Nguyen, A. M. Abbosh, and S. Crozier, "Thermo-dielectric breast phantom for experimental studies of microwave hyperthermia," *IEEE Antennas and Wireless Propagation Letters*, vol. 15, pp. 476-479, 2015.
- [19] T. M. Fiedler, M. E. Ladd, and A. K. Bitz, *SAR Simulations & Safety, NeuroImage*, vol. 168, pp. 33-58, 2018.
- [20] V. Sathiseelan, "Application of numerical modeling techniques in electromagnetic hyperthermia," *Applied Computational Electromagnetics Society (ACES) Journal*, vol. 7, no. 2, pp. 61-71, 2022.
- [21] T. Abouelnaga, I. Zewail, and M. Shokair, "Design of 10×10 massive MIMO array in sub-6 GHz smart phone for 5G applications," *Progress in Electromagnetics Research B*, vol. 91, pp. 97-114, 2021.



Mazhar Basyouni Tayel was born in Alexandria, Egypt on Nov. 20th, 1939. He graduated from Alexandria University Faculty of Engineering Electrical and Electronics department in 1963. He has published many papers and books in electronics, biomedical, and measurements.

Mazhar Basyouni Tayel received a B.Sc. with an honor degree in 1963, and then his Ph.D. in Electro-physics in 1970. He had this Prof. Degree of the elect. And communication and Biomedical Engineering and systems in 1980. Now he is Emeritus Professor since 1999. From 1987 to 1991 he worked as the chairman of the communication engineering section of EED BAU-Lebanon, and from 1991 to 1995 he worked as Chairman of the Communication Engineering Section, of EED Alexandria University, Alexandria, Egypt. Also from 1995 to 1996, he worked as a chairman of the EED Faculty of Engineering, BAU-Lebanon. Additionally, from 1996 to 1997, he worked as the Dean of the Faculty of Engineering, BAU - Lebanon. From 1999 to 2009, he worked as a senior professor in the Faculty of Engineering, Alexandria University, Alexandria, Egypt. He has been an Emeritus Professor at the Faculty of Engineering, Alexandria University, Alexandria, Egypt since 2009. He has also worked as a general consultant in many companies and factories and is a member of the supreme consul of Egypt.



Tamer Gaber Abouelnaga was born in November 1976. He received his B.Sc. degree (1994–1999, honors degree) in Electronics Engineering from Menofiya University, Egypt, an M.Sc. degree (2002–2007), and a Ph.D. degree (2007–2012) in Electronics and Communications from Ain Shams University. He works as a Researcher (2012–2017) and an Associate Professor (2018-current) in Microstrip Circuits Department at the Electronics Research Institute in Egypt. He works as Students Affairs Vice Dean (2018–2019) and Community Service, Environmental Development Vice Dean (2019-2022) at the Higher Institute of Engineering and Technology in Kafr Elsheikh, and Students Affairs Vice Dean (2022-2023) at the College of Industry and Energy Technology, New Cairo Technological University (NCTU), Egypt. He has published 42 papers, 29 papers in peer-refereed journals and 13. papers in international conferences regarding antennas, couplers, filters, and dividers for different microwave applications.



Nehad Mohamed Badran is a Master's Student at the Faculty of Engineering at Alexandria University, Egypt. She was born in El-Beheira, Egypt in December 1990. She received a B.Sc. degree in Electronics and Communication Engineering from HIET, Kafr El-Shiekh, Egypt in May 2012. She has been a demonstrator at the Higher Institute of Engineering and Technology (HIET) in Kafr El-Shiekh, Egypt since 2013. Her current research focus is Biomedical Engineering, especially microwave breast cancer detection and treatment.